

Study of Photoinduced *N*-Hydroxy-arylnitroxide Radicals (ArNO•OH) by Time-Resolved EPR

Vincent Maurel, Jean-Marie Mouesca,* Gérard Desfonds, and Serge Gambarelli*

Département de Recherche Fondamentale sur la Matière Condensée, Service de Chimie Inorganique et Biologique, CEA-Grenoble, 17 Avenue des Martyrs, 38054 Grenoble CEDEX 9, France

Received: September 28, 2004

The photoreduction of aromatic nitro compounds by alcohols is a well-known reaction; however, the first stages of its mechanism remain controversial. This study aims at characterizing the “primary” radicalar transients involved in this reaction by EPR spectroscopy. Laser flash photolysis ($\lambda = 266$ nm) of nitrobenzene, 5-nitouracil, *p*-nitroacetophenone, *o*-propylnitrobenzene, and 2-nitroresorcinol in ethylene glycol was followed by time-resolved EPR spectroscopy. In all reported TR-EPR spectra, except those obtained from the photolysis of 2-nitroresorcinol, the key intermediate *N*-hydroxy-arylnitroxide radicals (ArNO•OH, **1–4**) could be identified unambiguously. In 2-nitroresorcinol, the radical anion (ArNO•O⁻, **5**) and a σ iminoxy radical (**6**) were observed, and a third radical (**7**) remains unidentified. These observations indicate that two radicalar mechanisms (by H• transfer and by electron transfer) are competing in the photoreduction mechanism. The attribution of the EPR spectra was helped by DFT calculations of the hyperfine coupling constants (hcc's).

1. Introduction

Photoredox reactions of aromatic nitro compounds are among the most investigated photochemical reactions. These reactions can be intermolecular, such as the photoreduction of aromatic nitro compounds by alcohols,¹ or intramolecular.^{2,3} The latter possibility opens a wide range of applications, such as designing photolabile protecting groups⁴ and photoprecursors of active compounds, for example, DNA lesions^{5,6} and photoprecursors of neurotransmitters.⁷ In many cases, authors who reported these reactions invocated the abstraction of a hydrogen atom by the nitro moiety as the first step of the chemical mechanism (Scheme 1).

Few studies of the key ArNO•OH intermediates have been reported to date. The UV spectrum of PhNO•OH was reported by flash photolysis,^{8,9} but the attribution of the observed spectrum to this radical remained tentative. The PhNO•OH radical has been studied by mass spectrometry,¹⁰ but the observed reactivity is specific to the gas phase and the radical is produced by collision with charged particles and not by photochemistry. The *N*-muoxy phenylnitroxide¹¹ analogue of the PhNO•OH radical was reported by muon spin resonance. However, it was not produced photochemically and is not, strictly speaking, an ArNO•OH radical. Several steady-state EPR studies of the photochemistry of aromatic nitro compounds were reported, but in most of them only the anion radical ArNO•O⁻ or secondary radicals (ArNO•H, ArNO•R, and ArNO•OR) were observed.^{1,3,12–14} Only two ArNO•OH radicals have been reported by steady-state EPR studies: 2,3,5,6-(Cl)₄-PhNO•OH^{15,16} and 4-CN-PhNO•OH.¹⁷ Several authors have reported EPR spectra which they attributed to PhNO•OH^{13,18} but were later discovered to be spectra of PhNO•OR radicals.¹⁹

The aim of this study is to investigate the photoreactivity of aromatic nitro compounds in solution and to check the hypothesis of the exchange of H• between the aromatic nitro compound

(acceptor) and the solvent (donor). Among all the above cited methods, EPR is the most appropriate for the unambiguous detection of radicals. However, steady-state EPR is too slow for the observation of ArNO•OH radicals, whereas time-resolved EPR (TR-EPR) allows for the detection of radicals as soon as 100 ns after their formation by the laser pulse.^{20–23} This time scale should allow the unambiguous observation of radicals produced by the postulated exchange of H•. Ethylene glycol, a good donor of H•, was chosen as a solvent and the photolysis was carried out in neutral pH conditions. The choice of pH conditions is significant as a previous TR-EPR study of the photolysis of aromatic nitro compounds in basic conditions (2-propanol containing triethylamine) led to the detection of ArNO•O⁻ radicals.²⁴

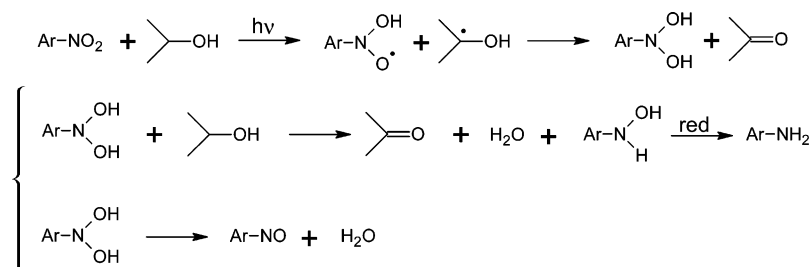
A series of experiments involving different aromatic nitro compounds (nitrobenzene, nitrobenzene-*d*₅, *p*-nitroacetophenone, *o*-propylnitrobenzene, 2-nitroresorcinol, 2-nitro-4,6 dideuterioresorcinol, and 5-nitouracil) were performed to determine the EPR features of ArNO•OH radicals and to observe the potential influence of the substituting groups on the reactivity of the parent compounds.

The attribution of TR-EPR spectra reported here was confirmed by ab initio calculations of the hyperfine coupling constants (hcc's). The DFT method of calculations was first validated on EPR spectra of radicals previously described in the literature.^{12–17,25}

2. Experimental Section

TR-EPR Experiments. TR-EPR experiments were performed using a Varian E102 EPR spectrometer. The spectrometer was operated in direct detection by removing the 100 kHz field modulation and the lock-in detection.²⁶ The EPR signal was observed via a large band preamplifier (bandwidth 100 MHz, Intercept, Elhyte Company) and a numerical oscilloscope (bandwidth 400 MHz, DSA 601A, Tektronix Company). Magnetic field measurements were performed using a Bruker ER 035M Gaussmeter.

* Address correspondence to these authors. E-mail: gambarelli@drfmc.ceng.cea.fr; mouesca@drfmc.ceng.cea.fr.

SCHEME 1: Mechanism of the Photoreduction of Aromatic Nitro Compounds by Alcoholic Solvents under Neutral Conditions¹

The solution under observation was continuously circulated through a quartz suprasil flat cell (optical path 0.3 mm) at a rate of 0.5 mL/min. Solution concentrations were adjusted to obtain an optical absorbance of 1.0 ($\lambda = 266$ nm) for a 0.3-mm optical path. The flat cell was placed in the microwave cavity of the EPR spectrometer (Varian E-238 mode TM110, with optical window). The solution was irradiated by the beam of an Nd:YAG pulsed laser ($\lambda = 266$ nm, pulse width = 5 ns, energy = 20 mJ/pulse, repetition rate = 10 Hz, Quantel B, Quantel Company, France). The surface of the cell irradiated by the laser beam was 27 mm². Laser pulsing and EPR detection were synchronized using a pulse generator (DG535, Stanford Research Company). In these conditions, the solution has received 10 laser flashes before leaving the irradiated area of the flat cell. The time response of the system was limited to 100 ns because of the quality factor of the filled cavity.

For each value of the magnetic field (0.1 G increment), the evolution over time of the EPR signal was recorded 64 times and summed. A blank was recorded by setting the magnetic field at a signal-free value and recording and summing 64 other time-resolved signals. For each value of the magnetic field, the measured blank and the continuous component were subtracted from the signal. The whole TR-EPR spectrum is obtained as a set of signals for different values of the magnetic field. Measurements and treatments were performed using in-house software programmed in LabView 5.1 (National Instrument). Another in-house program was used to simulate the spectra as sums of Gaussian curves. Chemically induced dynamic electron polarization (CIDEP) effects^{20,21,27–29} were not taken into account by this program.

Nitrobenzene, 2-nitroresorcinol, *o*-propylnitrobenzene, and *p*-nitroacetophenone were purchased from the Aldrich Company, 5-nitrouracil from the Fluka Company, and nitrobenzene-*d*₅ (99 at. % D) from the CEA, Service des Molécules Marquées, France. All these compounds were of the highest available purity and were used without further purification. Synthesis grade ethylene glycol was purchased from the SDS Company (France).

2-Nitro-4,6-dideuterioresorcinol. A solution of 250 mg of 2-nitroresorcinol in 6 mL D₂SO₄:D₂O (1:2) was stirred and refluxed for 8 h. Then, 14 mL of D₂O was added and the solution was refluxed for 16 h. The crude was taken up in Et₂O and washed with H₂O. This reaction had a 91% yield, ¹H NMR (200 MHz, CD₃OD): δ 7.18 ppm (s, 1H, C5). Electrospray MS, $m/z = 156.5$ ($[\text{M} - \text{H}]^+$). For the commercial protonated 2-nitroresorcinol, $m/z = 154.5$.

DFT Calculations. All the calculations rely on the use of the Amsterdam LCAO Density-Functional Programs (ADF 2.3) developed by Baerends and co-workers.^{30–35} We used the potential referred to as “VWN-BP”: Vosko, Wilk, and Nusair’s exchange and correlation energy^{36,37} completed by Becke’s³⁸ nonlocal gradient corrections to the exchange and by Perdew’s³⁹

corrections for the correlation. Those corrections were included in the self-consistent procedure. We used triple- ζ (plus polarization) basis sets for all atoms C, N, O, H, and Cl (unfrozen core orbitals).

3. Results and Discussion

A. TR-EPR Spectra Recorded during Photolysis of Aromatic Nitro Compounds. All of the aromatic nitro compounds investigated exhibited TR-EPR spectra. Figures 1, 2, and 3 show

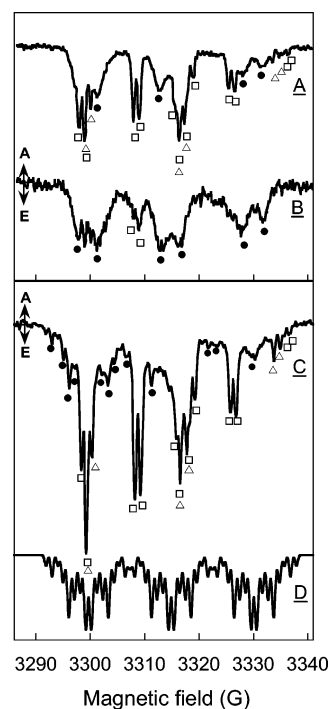


Figure 1. TR-EPR spectra recorded by flash photolysis of 5*d*-nitrobenzene (A and B) and nitrobenzene (C) and simulation for radical **1** (D). Concentration: 3.9 mM; microwave power: 20 mW; spectra A and C: average of signals measured from 200 to 1000 ns after the laser pulse; spectrum B: average of signals from 1000 to 1800 ns after the laser pulse (vertical scale expanded 3 times); spectrum D: simulated spectrum of radical **1** by a sum of Gaussian lines with hcc’s quoted in Table 2; filled circles radical **1** (in spectrum C) or **1d** (in spectra A and B); open squares radical **s1**, open triangles radical **s2**.

spectra obtained for nitrobenzene, 5-nitrouracil, and 2-nitroresorcinol, respectively. The polarization of all the spectra is mainly emissive because of a triplet CIDEP mechanism. For nitrobenzene, *o*-propylnitrobenzene, and *p*-nitroacetophenone, a small contribution of radical pair CIDEP mechanism is observed.^{20,21,27,29} In all TR-EPR experiments, we distinguished between two kinds of signals.

Radicals Derived from the Solvent (Ethylene Glycol). Some signals decay with a characteristic time (noted τ , determined

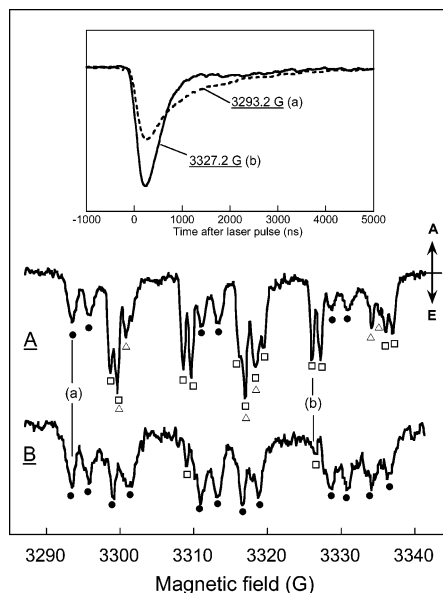


Figure 2. TR-EPR spectra recorded by flash photolysis of 5-nitouracil. Concentration: 9.0 mM; microwave power: 20 mW; spectrum A: average of signals measured from 350 to 600 ns after the laser pulse; spectrum B: average of signals from 1100 to 1350 ns after the laser pulse (vertical scale expanded 3 times); filled circles radical **2**, open squares radical **s1**, open triangles radical **s2**; inset: TR-EPR signals at 3293.2 G (a) attributed to radical **2** and at 3327.2 G (b) attributed to radical **s1** (signals averaged over a 1 G magnetic field window and a 250-ns time window).

by monoexponential fitting) shorter than 500 ns. These signals were attributed to two radicals, quoted as **s1** (marked by open squares in Figures 1–3) and **s2** (marked by open triangles), which are derived from ethylene glycol. The spectrum of **s1**, composed of 12 resolved lines, identifies **s1** as being HO–CH₂–C•H–OH upon comparison of the observed hcc's and the characteristic time decay τ value (see Table 1) with those reported in the literature.^{40–42} The spectrum of the radical **s2** is a triplet of doublets. Its hcc's (see Table 1) allow us to identify **s2** as being H₂C•OH by comparison with published data.^{40,41}

Radicals Derived from Aromatic Nitro Compounds. The other signals (filled circles in Figures 1 and 2, filled diamonds and asterisks in Figure 3) decay more slowly (see the inset in Figure 2) and were attributed to radicals derived from aromatic nitro compounds (see Table 2). This slower decay after the laser pulse allows the observation of radical spectra derived from aromatic nitro compounds at times when the signals of radicals **s1** and **s2** have almost disappeared (typically 1 μ s after the laser pulse, see Figures 1–3, spectra B). These spectra appeared to be composed of three main groups of lines of similar structures, which is consistent with a main hcc from a nitrogen nucleus. Assuming that the nitroaromatic compounds had produced the corresponding *N*-hydroxy-arylnitroxide radicals (ArNO•OH) **1–4** allows the interpretation of the spectra obtained by photolysis of nitrobenzene, 5-nitouracil, *p*-nitroacetophenone, and *o*-propylnitrobenzene. In the photolysis of 2-nitroresorcinol, the anionic nitro radical (ArNO•O[−]) **5** and two other radicals **6** and **7**, whose attribution is more tentative, were produced.

Nitrobenzene-*d*₅. The simplest spectrum, exhibiting a triplet of doublets, was obtained by photolysis of the nitrobenzene-*d*₅ (spectrum B in Figure 1). The hyperfine splitting due to deuterium atoms is unresolved. The hyperfine splitting of the doublets (3.35 G) is due to a nucleus with spin 1/2 (see Table 2) and none of the nuclei of nitrobenzene-*d*₅ has a spin 1/2. This observation and other arguments (see Identification section)

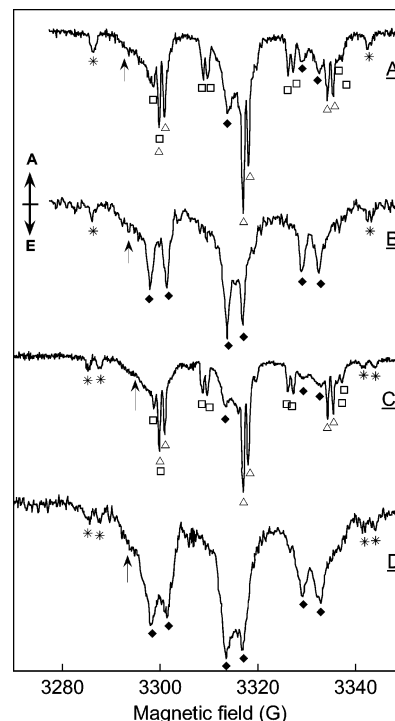


Figure 3. TR-EPR spectra recorded by flash photolysis of 2-nitro-4,6-dideoxiresorcinol (A and B) and 2-nitroresorcinol (C and D). Concentration: 12.9 mM; microwave power: 20 mW; spectra A and C: average of signals measured from 300 to 700 ns after the laser pulse; spectra B and D: average of signals from 1.1 μ s to 2.7 μ s after the laser pulse (vertical scale expanded 5 times); filled diamonds radical **5/5d**; asterisks radical **6/6d**; empty squares radical **s1**; empty triangles radical **s2**; vertical arrows: signal tentatively attributed to the ArNO•OH radical **7/7d** derived from 2-nitroresorcinol or 2-nitro-4,6-dideoxiresorcinol, respectively (see Identification section).

indicated that a hydrogen atom had been transferred from the solvent and added onto the nitrobenzene-*d*₅. The spectrum was thus interpreted as that of the radical **1d**. The influence of the energy of the laser pulses on the TR-EPR signal intensity was measured in a portion of the spectra recorded by photolysis of nitrobenzene-*d*₅ (see Supporting Information). Two groups of lines were studied: a doublet attributed to solvent radical **s1** and a large feature attributed to radical **1d**. In both cases, the TR-EPR signal is directly proportional to the pulse energy. This observation indicates that these radicals are produced via a monophotonic mechanism.

Nitrobenzene. The spectrum obtained by photolysis of nitrobenzene is more intricate (see Figure 1 spectrum C). We assumed that the radical observed **1** was similar to radical **1d** observed by photolysis of deuterated nitrobenzene and that hcc(N) and hcc(H_{NOOH}) measured in radical **1d** were similar in **1**. We then determined hyperfine coupling constants for the aromatic protons of radical **1** (see Table 2) by comparing the measured spectrum with a simulated one (see Figure 1 spectra C and D). The hcc's obtained for aromatic protons appeared similar to those given in the literature for aromatic protons of ArNO•OR radicals^{3,12,14,25} (see Tables 2 and 3).

5-Nitouracil. The spectrum recorded after photolysis of 5-nitouracil (see spectrum B in Figure 2) is composed of 12 (3 × 2 × 2) lines of equal intensity. They could easily be assigned to the radical **2** (hcc's in Table 2).

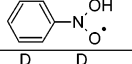
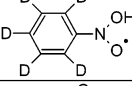
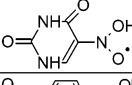
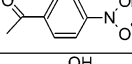
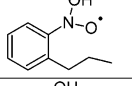
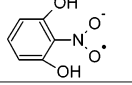
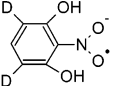
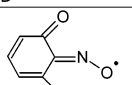
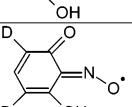
***p*-Nitroacetophenone.** The spectrum recorded by photolysis of *p*-nitroacetophenone (see Supporting Information) qualitatively allows for its identification (radical **3**). The easy data simulation yields the corresponding hcc's (see Table 2).

TABLE 1: Experimental hcc's (G), Landé Factor *g*, and Characteristic Time Decay τ (ns) for Radicals Derived from Ethylene Glycol

	radicals	H(C α)	H(C β)	H(OH-C α)	γ	τ
s1	HO-CH ₂ -C•H-OH	17.5, 1H	9.9, 2H	1.0, 1H	2.00308 (5) ^a	410 (+/-100)
s2	H ₂ COH	17.2, 2H		1.1, 1H	2.00332 (6+5) ^{b,c}	<500 ^d

^a From ref 42. ^b Determined taking the signal of **s1** as a reference. ^c Uncertainty on the *g* value is given as uncertainty in this work + uncertainty of the radical **s1** used as a reference.⁴² ^d This value cannot be measured accurately, because all spectra lines corresponding to radical **s2** are superimposed on lines of other radicals.

TABLE 2: Experimental hcc's (G) and DFT Calculated hcc's (in Italics) for Radicals Observed in TR-EPR Experiments (This Work)^k

Radical	type ^a	N	H _{NOOH}	H _{ortho}	H _{meta}	H _{para}	Other	<i>g</i> ^b
1 	π	15.2	3.35	3.05	1.1	4.0	-	2.00461(6+5) ^c
	π	6.2	-1.3	-3.5	1.1	-4.1	-	
1d 	π	15.2	3.35	u	u	u	-	2.00456(6+5) ^c
	σ^*	17.5	2.3	-	-	-	5.5 ^d	2.00477(6+5) ^c
	σ^*	13.2/21.5 ^e	-1.2/19.9 ^e	-	-	-	-4.6/-6.9 ^e	
2 	π	5.3	-1.7	-	-	-	-10.7	
	π	13.0	3.1	3.2	1.1	-	-	2.00483(6+5) ^c
3 	π	5.4	-1.3	-3.2	1.0	-	-	
	π	14.5	u	u	u	u	u ^f	- ^g
4 	π	6.25	-1.1	-3.7	1.0	-4.2	6.4, 2H ^f	
	π	15.5	-	-	u	3.3	u ^h	2.00465(10+5) ^c
5 	π	15.6	-	-	0.99	3.41	0.34 ^h	2.00463
	Ref ⁱ							
5d 	π	15.5	-	-	u	3.3	u	2.00473(10+5) ^c
6j 	σ	28.2	-	-	2.3, 1H	u	-	2.00506(10+5) ^c
	σ	28.2	-	-	u	u	-	2.00513(10+5) ^c
6d ^j 	σ	28.2	-	-	u	u	-	2.00513(10+5) ^c

^a See Results section. ^b Determined taking the signal of **s1** as a reference. ^c Uncertainties on the last digits of the *g* values given as uncertainty in this work + uncertainty of the radical **s1** used as a reference.⁴² ^d H in C6 of the uracil moiety. ^e Minimum and maximum of hcc values calculated for $\beta = 45^\circ$ (see Identification section). ^f This hcc corresponds to protons on the carbon α of the propyl group; it is calculated for the optimized geometry and does not take the rotation of the propyl group into account. ^g Not measurable. ^h Two equivalent protons of hydroxyl groups. ⁱ Experimental hcc's and *g* from ref 43. ^j Putative radical **1**; see Identification section for the computed hcc values ^k u = unresolved hcc.

o-Propylnitrobenzene. The spectra recorded after photolysis of *o*-propylnitrobenzene exhibited three very large features (width around 10 G) in addition to the now familiar signals of radicals **s1** and **s2**. It only allowed for the determination of the hcc of the nitrogen atom identified as being that of radical **4** (see Table 2 and spectra in the Supporting Information).

2-Nitroresorcinol. The spectra recorded after photolysis of 2-nitroresorcinol differ from the other spectra described so far in this study. These spectra (see Figure 3 spectra C and D) show two kinds of signals in addition to those attributed to radicals **s1** and **s2**. A first signal is composed of large features and exhibits a triplet of doublets: hcc(N) = 15.5 G, hcc(H) = 3.3 G. This signal was attributed to the radical anion **5** (filled diamonds in Figure 3C and D) derived from 2-nitroresorcinol by comparison with a spectrum recorded during the radiolysis of 2-nitroresorcinol in aqueous solution.⁴³ The second signal appears as two doublets at both extremities of the spectra. These doublets (hcc(H) = 2.3 G) are still observed one microsecond after the laser pulse, but their intensity is very weak compared to that of the signal attributed to radical **5**. They were attributed to another radical derived from 2-nitroresorcinol noted **6**

(asterisks in Figure 3C and D). This hypothesis of two different radicals is confirmed by modifications observed in the corresponding spectra in the experiment on deuterated 2-nitroresorcinol (see next paragraph). The hypothetical feature of **6** in the central part of the spectra could not be identified unambiguously probably because of the stronger intensity of the signal of **5**. The identification of radical **6** remains tentative and will be discussed on the basis of DFT calculations (see Identification section). An unresolved signal indicated by an arrow in Figure 3 is probably due to a third radical (called **7**) derived from 2-nitroresorcinol (see Identification section).

2-Nitro-4,6-dideuterioresorcinol. When this compound is photolyzed in the same conditions, the signal attributed to the radical **5d** (filled diamonds in Figure 3A and B) exhibits unchanged hyperfine splitting constants, compared to the radical **5** (see Figure 3 spectra B and D). This supports the attribution of radical **5** as being the radical anion derived from 2-nitroresorcinol. In the same experiment, signals attributed to radical **6d** (asterisks in Figure 3A and B) do not exhibit the hcc of 2.3 G measured for the radical **6**. So in this latter radical, hydrogen atoms 4 and 6 are not equivalent and only one of them produces

TABLE 3: Experimental hcc's of Radicals Previously Reported in the Literature and Corresponding DFT Calculated hcc's (in Italics, This Work)ⁱ

radical	type	N	<i>H</i> _{ortho}	<i>H</i> _{meta}	<i>H</i> _{para}	other <i>H</i>
a 2,3,5,6-(Cl) ₄ -PhNO•OH ^a	<i>σ</i> [*]	23.1/23.9 27.1			u -0.4	3.8/4.7, NO•OH -0.9
b <i>p</i> -CN-PhNO•OH ^b	<i>π</i>	12.2 5.4	3.2 -3.3	1.1 1.0		3.2, NO•OH -1.4
c PhNO•H ^c	<i>π</i>	9.1 3.4	2.8 -3.1; -2.7	1.0 0.9	3.2 -3.5	12.1, NO•H -11.4
d PhNO•OR ^{c,d}	<i>π</i>	15.0/15.2 6.2	2.9/3.0 -3.3; -3.2	1.0 1.0	3.0/3.2 -3.8	-0.6; -0.5; -0.4, CH ₃ ^e
e PhNO•R ^{c,d,f}	<i>π</i>	10.5/11.8 4.5	3.0 -3.0; -2.7	1.0 0.9	3.0 -3.8	-14.7; -14.5; -0.3, CH ₃ ^e
f <i>p</i> -CN-PhNO•H ^b	<i>π</i>	8.2 2.9	3.1; 2.7 -3.0; -2.6	1.1 0.9		11.3, NO•H -10.7
g 3,5-(NO ₂) ₂ -PhNO•R ^d	<i>π</i>	9.7 3.9	2.6 -2.6; -3.3		2.6 -3.7	14.1; 14.1; -0.3, CH ₃ ^e
h 3,5-(NO ₂) ₂ -PhNO•OR ^d	<i>π</i>	13.3 5.4	3.0 -3.0; -3.6		3.0 -4.1	-0.6; -0.6; -0.2, CH ₃ ^e
i 3-Cl-PhNO•OR ^{g,h}	<i>π</i>	14.2 6.0	3.0 -3.5	1.1 1.0	3.0 -4.1	
j 4-Cl-PhNO•OR ^{g,h}	<i>π</i>	14.5 6.0	3.1 -3.5	1.1 1.1		

^a See refs 15, 16. ^b See ref 17. ^c See ref 12. ^d See ref 14. ^e These calculations for ArNO•OR were performed with R=CH₃ even when experimental data correspond to other moieties. ^f See ref 13. ^g See ref 25. ^h Our calculations yield very close hcc(N) and hcc(H_{arom}) values for ArNO•OH and ArNO•OR radicals derived from the same nitroaromatic compound. Calculations were performed for ArNO•OH radicals and compared to the experimental data of the corresponding ArNO•OR radicals. ⁱ In cases where several experimental references are available, minimum and maximum of each hcc value are quoted as "min/max". When protons are found nonequivalent, their quoted hcc values are separated by ";". u = unresolved hcc.

the doublets (hcc(H) = 2.3 G) observed in the photolysis of protonated 2-nitroresorcinol. The unresolved signal of **7d** indicated by an arrow in Figure 3 is not notably changed compared with the spectra of **7** obtained with protonated 2-nitroresorcinol.

B. Identification of the Radicals. Identification of Radicals 1, 3, and 4. The experimental evidence (especially the isotopic substitution, see above) are sufficient to identify radical **1** as being PhNO•OH, whose experimental spectra (see Figure 1) are reported here. In radical **3**, the experimental procedure and the qualitative analysis of the corresponding spectra also naturally lead to its identification. Such is not the case however for radical **4** which is only identified by analogy, as the spectral data are insufficient by themselves (only a hcc(N) value of 14.5 G can be deduced). We identify these three radicals **1**, **3**, and **4**, with reasonable certainty, as being of the ArNO•OH type. Two other radicals of similar chemical structure have been reported in the literature (see Table 3, radicals **a**^{15,16,25} and **b**¹⁷). One of these (**b**: *p*-CN-PhNO•OH) possesses an hcc value of 12.15 G, comparable to those of radicals **1**, **3**, and **4**, comprised between 13.0 and 15.2 (see Table 2) whereas the other one (**a**), derived from a tetrachloro-nitrobenzene, exhibits a much larger hcc for the functional nitrogen atom (23.1¹⁵/23.9 G¹⁶). This observation illustrates the influence of chemical substitution, especially at the ortho position, on the conformation around the nitrogen atom and on its hcc.⁴³⁻⁴⁷

It could be tempting to try to harmonize the experimental data available for **1**, **3**, and **4** within the ArNO•OH family with the help of DFT calculations. Since no crystallographic structures are available for the radicals considered here, hcc's would have to be computed only after full geometry optimization. A preliminary geometry optimization DFT computation in vacuo of the radical **1** yields a planar geometry around the nitrogen group (*π* radical), already reported in the literature using B3LYP calculations,¹⁰ or semiempirical PM3 method.¹¹ This planar conformation results in a rather disappointing value of hcc(N) = 6.2 G (against 15.2 G experimentally, cf. Table 2). Ring (ortho, meta, para) protons' hcc's (3.5, 1.1, 4.1 G) by contrast

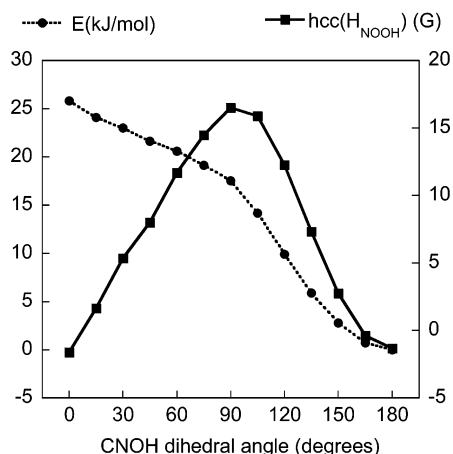


Figure 4. Variations of total energy and of hcc(H_{NOOH}) with the dihedral angle C-N-O-H in radical **1** PhNO•OH. For each point, the conformation of the PhNO•OH radical was DFT calculated by monitoring the dihedral angle C-N-O-H and by optimizing all other internal coordinates. The calculated energetic barrier for the rotation of the O-H bond around the N-O bond (25.8 kJ•mol⁻¹) is of the order of magnitude of a hydrogen bond in alcohols.

are very satisfying (3.05, 1.1, 4.0 G experimentally) whereas the computed hcc (-1.6 G) for the proton of the NO•OH group, located in the aromatic plane, was significantly lower than the experimental one (3.35 G). The rotation of the OH bond around the corresponding NO bond in the NO•OH group strongly affects the hcc value (between -1.6 and 16.5 G, see Figure 4).⁴⁸

This preliminary attempt serves to illustrate that great caution has to be taken when dealing with *π* radicals, such as radicals **1**, **3**, and **4**, for which the unpaired electron lies in an orbital *perpendicular* to the plane defined by the nitrogen and its nearest neighbors. This last feature results in the hcc values of the atoms lying in this plane being essentially determined by the spin polarization mechanism. This mechanism describes the differential interaction of the unpaired electron with the inner shell

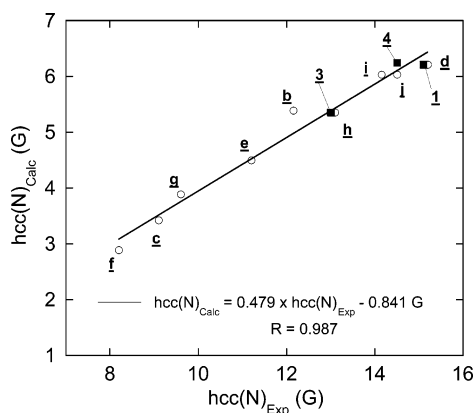


Figure 5. Calculated $hcc(N)$ vs experimental $hcc(N)$ for π radicals. The linear fit (least-squares method) takes into account only radicals previously described in the literature (open circles, letters as in Table 3); filled squares: ArNO•OH radicals (numbers as in Table 2) observed in this study.

spin-paired electrons, a subtle and indirect effect determinant for π radicals. This subtlety in itself explains the major discrepancy between computed and measured $hcc(N)$ values,^{46,49} as is the case for radical **1** (a discrepancy therefore also expected for radicals **3**, **4**, and **b**; see Tables 2 and 3). More generally, conventional calculations tend, for the same reason, to underestimate the absolute values of the nitrogen hcc in nitroxides using both Hartree–Fock and DFT methods.^{46,47}

The “state-of-the-art” way of proceeding further is well established in most cases. Quantum mechanical models have been developed which combine DFT unrestricted Kohn–Sham codes with the modeling of bulk solvent effects and vibrational averaging effects. More precisely, the use of hybrid exchange–correlation potentials (i.e., B3-LYP) has been proposed to improve the description of the spin polarization effect as well as composite approaches.⁵⁰ The solvent can be modeled as a dielectric continuum with or without explicit solvent molecules.⁵¹

Applying this whole methodology is beyond our goal as we aim simply to confirm the identification of the radicals we observe. Keeping that in mind, we think it best to check the consistency of our radicals experimental data (especially for **1**, here observed conclusively for the first time) with those of a series of π radicals of similar structure derived from aromatic nitro compounds **b–j** (ArNO•OH, ArNO•OR, ArNO•H, and ArNO•R; cf. Table 3) whose EPR spectra had already been reported in the literature. For this very restricted purpose, the computation in vacuo of $hcc(N)$ values, after geometry optimization, is amply sufficient, as will be shown.

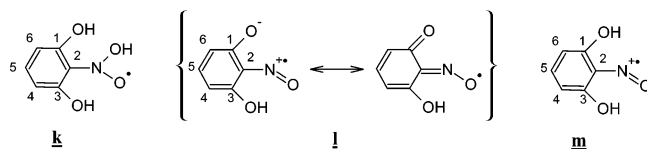
Calculated ($hcc(N)_{Calc}$) and experimental ($hcc(N)_{Exp}$) values for **b–j** radicals follow the same trend: $hcc(N_{NOH}) < hcc(N_{NOR}) < hcc(N_{NOOH}) \sim hcc(N_{NOOR})$. More precisely, both sets of values are linearly correlated (see Figure 5) through the following “ π correlation” (in Gauss):

$$hcc(N)_{Calc} = 0.479hcc(N)_{Exp} - 0.841$$

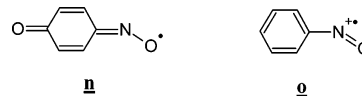
As can be verified in Figure 5, our three measured π radicals **1**, **3**, and **4** are well inserted within this π correlation. This strongly substantiates their identification.

Identification of Radical 6. Several structural hypotheses have been explored for radical **6**. The first to come to mind, following our work above on the ArNO•OH radicals, is the tentative radical **k** (see Scheme 2). Its geometry optimization yields a σ^* radical⁵² (i.e., pyramidalized N) with computed $hcc(N) =$

SCHEME 2: Hypotheses for the Structure of Radical 6



SCHEME 3: Chemical Structures of Radicals n (Model of l) and o (Model of m)



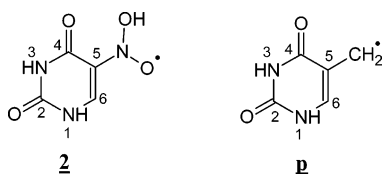
23.8 G. This geometry is constrained by two internal hydrogen bonds between the hydrogen atoms of the hydroxyl groups and the oxygen atoms of the functional group. We had already noticed such a pyramidalization of the functional NO•OH group when both ortho positions are occupied by chlorine atoms (preliminary results), as was the case of radical **a** for which experimental $hcc(N)$ equals 23.1 G.¹⁵ However, the computed hcc 's for aromatic protons of **k** ($hcc(H_{C4}) = 0.9$ G, $hcc(H_{C5}) = -2.5$ G, $hcc(H_{C6}) = 0.5$ G) are definitely not compatible with the experimental ones for radical **6** (see Table 2, the para $hcc(H_{C5})$ is extinguished whereas the two meta H_{C4} and H_{C6} exhibit different hcc 's).⁵⁶

The next most probable guess is the neutral radical **l**, possibly resulting from an intramolecular dehydration of the primary ArNO•OH radical **k** and its protonated form **m**.

Radical **l** is a member of the iminoxy radicals of σ type.^{57,58} In the literature,⁵⁸ we find the related iminoxy radical **n**, a simpler model of **l**, that is, without the hydroxy groups in ortho positions (see Scheme 3), for which two $hcc(H)$'s have been measured, one at 3.7 G and one at 1.2 G, in addition to $hcc(N) = 33.0$ G. We checked our DFT procedure in vacuo on this radical and obtained $hcc(N) = 32.5$ G, one $hcc(H_{meta})$ at 5.7 G, and $hcc(H_{ortho})$ at -1.0 G. We therefore confidently computed the $hcc(H)$ at the same DFT level for radical **l**. However, as the calculated hcc 's were sensitive to the local hydroxyl conformations, a set of four representative planar conformations has been tested (OH groups toward/away from the NO group: see Supporting Information). In all conformations, meta protons are found nonequivalent. The $hcc(H_{para})$'s are lower than 1.5 G for three of the four conformations studied. In addition, the $hcc(N)$'s are comprised between 16.6 and 34.1 G. These DFT results are compatible with our experimental data.

Radical **m**, a protonated form of **l**, is a member of the nitroso cation radical family. The literature provides us with measured hcc 's for a simpler (without hydroxy groups) model of **m**, the nitrosobenzene PhNO•⁺ cation radical **o**⁵⁹ (for EPR spectra of similar radicals, see ref 57). Its $hcc(N)$ is very high (37.0 G) and the only other resolved hcc is due to one meta proton (3.8 G). Our computation of the proton hyperfine constants for radical **o** reproduces the nonequivalency of the two meta protons (5.3 and -0.2 G). We also found $hcc(N) = 34.5$ G. We therefore confidently computed the $hcc(H)$'s at the same DFT level for radical **m**, following the same procedure as for **l**, defining four planar conformations depending on the hydroxyl orientations. The hcc 's analysis is qualitatively similar (see Supporting Information) to that of radical **l**, though for **m**, computed $hcc(N)$ is always greater than 29 G.

As for choosing between neutral **l** and cationic **m**, one clue may be given by Gronchi and Tordo's work⁵⁷ (see also ref 60) which mentions that iminoxy radicals tend to have larger g values (about 2.005) than their cationic counterparts (about

SCHEME 4: Chemical Structures of Radicals 2 and p

2.002). This tentative argument would plead in favor of **1** over **m** as being our radical **6**, hence our proposal in Table 2. More cannot be said at this level of analysis.

Identification of Radical 2. The experimental $\text{hcc}(\text{N}_{\text{NOOH}})$ value of 17.5 G suggests an $\text{ArNO}\cdot\text{OH}$ radical. Geometry optimization for radical **2** yields a π radical exhibiting an intramolecular hydrogen bond between the hydrogen atom of the $\text{NO}\cdot\text{OH}$ group and the oxygen atom of the nearest carbonyl group. In this planar conformation, the computed hyperfine constant $\text{hcc}(\text{H}_{\text{C}_6}) = -10.7$ G is very different from the experimental splitting constant (5.5 G, see Table 2). To check the accuracy of this calculated $\text{hcc}(\text{H}_{\text{C}_6})$, we considered a similar radical formed by loss of a hydrogen atom from the methyl group of the thymine (**p**). The $\text{hcc}(\text{H}_{\text{C}_6})$ has been measured to be in the range $[-10.2$ G; -11.3 G]^{61–63} and has been computed by DFT B3-LYP (-11.4 G).⁶⁴ We satisfactorily computed it to be -10.6 G (π radical). The experimental value of 5.5 G for the same proton in radical **2** therefore excludes a π conformation and suggests that the result of the geometry optimization in vacuo is probably not the most stable conformation of radical **2** in a solution of ethylene glycol.

Explicitly modeling the solvent being beyond the scope of this paper, we explored a two-dimensional conformational space defined by the two monitored dihedral angles $\text{C}_5\text{--N--O--H}$ (noted α) and $\text{C}_4\text{--C}_5\text{--N--OH}$ (noted β), ranging from 0° to 360° and from 0° to 180° , respectively. We found one region of the conformational space (β about 45°) for which the computed $\text{hcc}(\text{N}_{\text{NOOH}})$ is about 18 G and $\text{hcc}(\text{H}_{\text{C}_6})$ is about -6 G (Supporting Information Figure S4). For this β value, $\text{hcc}(\text{N}_{\text{NOOH}})$ varies between 13.2 G to 21.5 G, with α varying in the $0\text{--}360^\circ$ range, while $\text{hcc}(\text{H}_{\text{C}_6})$ varies between -4.6 and -6.9 G (Supporting Information Figure S5). These ranges are consistent with the corresponding experimental values (17.5 and 5.5 G, respectively). Moreover, for these conformations defined by β about 45° , radical **2** is a σ^* radical (see Table 2). We have some confidence in the computed $\text{hcc}(\text{N})$ values of this σ^* radical as, for simpler $\text{R--NO}\cdot\text{OH}$ σ^* radicals derived from aliphatic nitro compounds ($\text{MeNO}\cdot\text{OH}$ and $\text{EtNO}\cdot\text{OH}$), the computed values for $\text{hcc}(\text{N})$, 30.3 and 29.9 G, respectively,

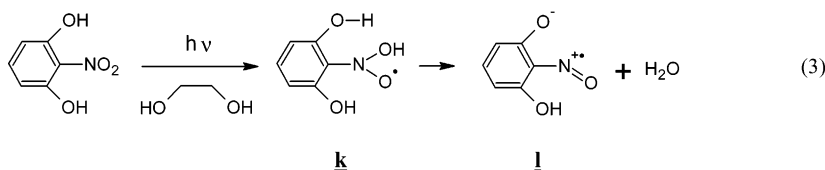
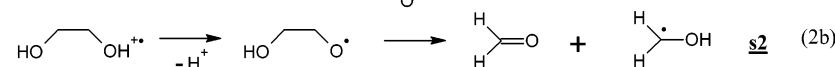
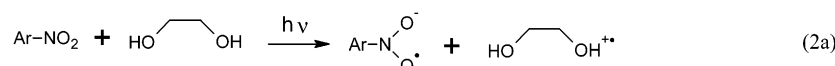
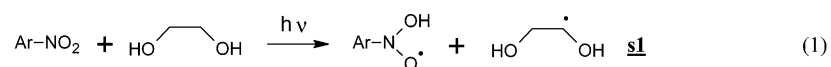
compare well to the experimental values, 28.2 and 28.0 G, respectively.^{65,66}

The putative σ^* conformation for radical **2**, along with the relatively high $\text{hcc}(\text{N})$ value of 17.5 G, is probably linked to the presence of the $\text{C}=\text{O}$ bond at position 4. This $\text{C}=\text{O}$ group is highly polarized and therefore tightly surrounded by solvent molecules. This “steric effect” may induce a conformational change of the $\text{NO}\cdot\text{OH}$ group from π (in vacuo) to σ^* (in solvent). The same phenomenon (steric effect) is operative in the *o*-Cl-PhNO•OR exhibiting an experimental $\text{hcc}(\text{N})$ value of 17.5 G²⁵ whereas the *m*-Cl-PhNO•OR (**i**) and *p*-Cl-PhNO•OR (**j**) π radicals present $\text{hcc}(\text{N})$ values at 14.2 and 14.5 G, respectively (see Table 3). This effect is further enhanced when both ortho positions are occupied by bulky substituents as in radical **a** (2,3,5,6-(Cl)₄-PhNO•OH) with $\text{hcc}(\text{N}) \approx 23.5$ G.¹⁵

C. Chemical Mechanisms. The TR-EPR study described here provides several points of evidence showing that the primary photochemical act is a hydrogen abstraction from ethylene glycol by an excited triplet state in the four different aromatic nitro compounds, producing $\text{ArNO}\cdot\text{OH}$ radicals **1–4** and **s1**.

(i) The EPR spectrum of radicals $\text{ArNO}\cdot\text{OH}$ **1–4** were identified in the TR-EPR signal recorded after the photolysis of corresponding aromatic nitro compounds in ethylene glycol. Their attribution was confirmed by DFT calculations of hyperfine splitting constants. (ii) In the same TR-EPR experiments, the EPR spectrum of radical **s1** was identified, which establishes the abstraction of a hydrogen atom from the solvent. (iii) The EPR spectra of these radicals were both observed during the first microsecond following the laser pulse. (iv) The observed mechanism is monophotonic. (v) The pattern of the TR-EPR spectra, mainly emissive, indicates that the CIDEP effect occurs mainly via the triplet mechanism. It is consistent with the first step of the proposed mechanism, which involves an excited triplet state of the aromatic nitro compound.

Nevertheless, this mechanism does not explain the EPR spectra observed by photolysis of 2-nitroresorcinol. In particular, the anion radical **5** was identified as the major radical derived from 2-nitroresorcinol, in the TR-EPR spectra. In the same spectrum, one can notice that the signal due to the radical **s2** ($\text{H}_2\text{C}\cdot\text{OH}$) is notably intense compared with other TR-EPR spectra reported in this paper.⁶⁷ We thus propose a mechanism which can explain the formation of both radicals **s2** and **5**. The photoexcited aromatic nitro compound abstracts an electron from ethylene glycol, which produces the anion radical derived from

SCHEME 5: Proposed Mechanisms. H• Transfer (Reaction 1), Electron Transfer (Reaction 2a and 2b), and Formation of Radical 6 (=1, Reaction 3)

the aromatic nitro compound (see reaction 2a, Scheme 5). The cation radical of ethylene glycol then loses a proton, resulting in a neutral alkoxy radical, which decomposes by β -scission of the carbon–carbon bond (see reaction 2b, Scheme 5).

During the photolysis of all other aromatic nitro compounds (see Figures 1 and 2), one can see that the signal due to **s2** is weak compared to that of **s1**. This indicates that the mechanism of electron transfer is less important than the mechanism of H• transfer. The EPR spectra of anion radicals derived from aromatic nitro compounds are most probably too weak to be observed compared to that of ArNO•OH radicals **1–4**.

The formation of radical **6** remains to be explained. According to our DFT calculations, the most probable structure for this radical⁷² is **I** (see Schemes 2 and 3). We suggest that this species could be produced as follows: the H• transfer is followed by an intramolecular dehydration of the “primary” ArNO•OH radical (see reaction 3, Scheme 5). In this case, the unresolved signal of radical **7** could be a part of the spectrum of the ArNO•OH radical **k**.

These mechanistic considerations give a unified point of view for the photolysis of all aromatic nitro compounds reported in this paper: the H• transfer competes with the electron transfer. The H• transfer is favored in all cases but that of the photolysis of 2-nitroresorcinol (radicals **1–4**). In the latter case, the electron transfer is dominant (radical **5**), and the less important mechanism of H• transfer is followed by an intramolecular dehydration of the ArNO•OH radical (radical **6**).

4. Conclusion

The TR-EPR experiments reported in this study unambiguously characterize the key intermediates of the photolysis of aromatic nitro compounds. In particular, EPR spectra of ArNO•OH radicals **1–4** are reported. The interpretation of the EPR spectra was helped and confirmed by DFT calculations. A correlation set from these data was used when a direct comparison between calculated and experimental hcc values was not relevant (hcc of the functional nitrogen atom in π radicals). The observed radicals are rationalized by two competing mechanisms. The first mechanism is a H• transfer, dominant in all cases but that of 2-nitroresorcinol. The second mechanism, dominant in the photolysis of 2-nitroresorcinol, is most probably an electron transfer. The TR-EPR spectra recorded during photolysis of 2-nitroresorcinol suggest that the primary ArNO•OH reacts via an intramolecular dehydration. This kind of reactivity could be useful to design some photoinduced intramolecular reactions.

Acknowledgment. The authors gratefully acknowledge Pr. André Rassat and Dr. Josette Michon for helpful discussions, Colette Lebrun for technical assistance (mass spectrometry), and Dr. Maighread Gallagher for checking the English.

Supporting Information Available: As Supporting Information are given the following: **S1**, variations of the TR-EPR spectrum observed by flash photolysis of nitrobenzene-*d*₅ versus the energy of the laser pulse; **S2**, TR-EPR spectrum observed by flash photolysis of *p*-nitroacetophenone (with radical **3**); **S3**, TR-EPR spectrum observed by flash photolysis of *o*-propylnitrobenzene (with radical **4**); **S4**, calculated hcc's (G) for different planar conformations of the radicals **1** (neutral form) and **m** (cationic protonated form); **S5**, variations of hcc's of radical **2** with the dihedral angle β , C4–C5–N–O_H; **S6**, variations of hcc's of radical **2** with the dihedral angle α , C5–N–O–H. This

material is available free of charge via the Internet at <http://pubs.acs.org>.

References and Notes

- (1) Chow, Y. L. Photochemistry of Nitro and Nitroso Compounds, Part I, Chapter 6, Supplement F. In *The Chemistry of Amino, Nitroso and Nitro Compounds and Their Derivatives*; Patai, S., Ed.; John Wiley: New York, 1982.
- (2) Nakagaki, R.; Mutai, K. *Bull. Chem. Soc. Jpn.* **1996**, *69*, 261.
- (3) Corrie, J. E. T.; Gilbert, B. C.; Munasinghe, V. R. N.; Whitwood, A. C. *J. Chem. Soc., Perkin Trans. 2* **2000**, 2483.
- (4) Cameron, J. F.; Fréchet, J. M. J. *J. Am. Chem. Soc.* **1991**, *113*, 4303.
- (5) Kotera, M.; Roupioz, Y.; Defrancq, E.; Bourdat, A.-G.; Garcia, J.; Coulombeau, C.; Lhomme, J. *Chem. Eur. J.* **2000**, *6*, 4163.
- (6) Crey-Desbiolles, C.; Lhomme, J.; Dumy, P.; Kotera, M. *J. Am. Chem. Soc.* **2004**, *126*, 9532.
- (7) Wilcox, M.; Randall, W. V.; Johnson, K. W.; Billington, A. P.; Carpenter, B. K.; McCray, J. A.; Guzikowski, A. P.; Hess, G. P. *J. Org. Chem.* **1990**, *55*, 1585.
- (8) Asmus, K. D.; Wigger, A.; Henglein, A. *Ber. Bunsen-Ges. Phys. Chem.* **1966**, *70*, 862.
- (9) Iyer, S.; Capellos, C. Transient Photochemistry of Nitrobenzene and Nitronaphthalenes. In *Advances in Chemical Reaction Dynamics*; Rentzepis, P. M., Capellos, C., Eds.; Reidel: Amsterdam, 1986; p 405.
- (10) Polasek, M.; Turecek, F. *J. Am. Chem. Soc.* **2000**, *122*, 9511.
- (11) Rhodes, C. J.; Morris, H.; Scott, C. A.; Reid, I. D.; Roduner, E. *Magn. Reson. Chem.* **1997**, *35*, 357.
- (12) Wong, S. K.; Wan, J. K. S. *Can. J. Chem.* **1973**, *51*, 753.
- (13) Chachaty, C.; Forchioni, A. *J. Chim. Phys. Phys.-Chim. Biol.* **1968**, *65*, 1649.
- (14) Menapace, J. A.; Marlin, J. E. *J. Phys. Chem.* **1990**, *94*, 1906.
- (15) Cowley, D. J.; Sutcliffe, L. H. *Trans. Faraday Soc.* **1969**, *65*, 2286.
- (16) Sutcliffe, L. H. *J. Chem. Soc., Faraday Trans. 1* **1985**, *81*, 1467.
- (17) Levy, N.; Cohen, M. D. *J. Chem. Soc., Perkin Trans. 2* **1979**, 553.
- (18) Ward, R. L. *J. Chem. Phys.* **1963**, *38*, 2588.
- (19) Janzen, E. G.; Gerlock, J. L. *J. Am. Chem. Soc.* **1969**, *91*, 3108.
- (20) van Willigen, H.; Levstein, P. R.; Ebersole, M. H. *Chem. Rev.* **1993**, *93*, 173.
- (21) Turro, N. J.; Kleinman, M. H.; Karatekin, E. *Angew. Chem., Int. Ed.* **2000**, *39*, 4436.
- (22) Stehlik, D.; Möbius, K. *Annu. Rev. Phys. Chem.* **1997**, *48*, 745.
- (23) Forbes, M. D. E. *Photochem. Photobiol.* **1997**, *65*, 73.
- (24) Akiyama, K.; Ikegami, Y.; Ikenoue, T.; Tero-Kobuta, S. *Bull. Chem. Soc. Jpn.* **1986**, *59*, 3269.
- (25) Cowley, D. J.; Sutcliffe, L. H. *J. Chem. Soc. B* **1970**, 569.
- (26) McLauchlan, K. A. Time-resolved EPR. In *Advanced EPR, applications in biology and biochemistry*; Hoff, A. J., Ed.; Elsevier: Amsterdam, 1989; p 345.
- (27) McLauchlan, K. A. *J. Chem. Soc., Perkin Trans. 2* **1997**, 2465.
- (28) Jäger, M.; Norris, J. R. *J. Phys. Chem. A* **2002**, *106*, 3659.
- (29) Buckley, C. D.; McLauchlan, K. A. *Mol. Phys.* **1985**, *54*, 1.
- (30) Ziegler, T. *Chem. Rev.* **1991**, *91*, 651.
- (31) Baerends, E. J.; Ellis, D. E.; Ros, P. *Chem. Phys.* **1973**, *2*, 41.
- (32) Baerends, E. J.; Ros, P. *Chem. Phys.* **1973**, *2*, 52.
- (33) Baerends, E. J.; Ros, P. *Int. J. Quantum Chem., Quantum Chem. Symp.* **1978**, *12*, 169.
- (34) Bickelhaupt, F. M.; Baerends, E. J.; Ravenek, W. *Inorg. Chem.* **1990**, *29*, 350.
- (35) TeVelde, G.; Baerends, E. J. *J. Comput. Phys.* **1992**, *99*, 84.
- (36) Painter, G. S. *Phys. Rev. B: Condens. Matter* **1981**, *24*, 4262.
- (37) Vosko, S. H.; Wilk, L.; Nusair, M. *Can. J. Phys.* **1980**, *58*, 1200.
- (38) Becke, A. D. *Phys. Rev. A* **1988**, *38*, 3098.
- (39) Perdew, J. P. *Phys. Rev. B: Condens. Matter* **1986**, *33*, 8822.
- (40) Livingston, R.; Zeldes, H. *J. Chem. Phys.* **1966**, *44*, 1245.
- (41) Trifunac, A. D.; Thurnauer, M. C. *J. Chem. Phys.* **1975**, *62*, 4889.
- (42) Jäger, M.; Norris, J. R. *J. Magn. Reson.* **2001**, *150*, 26.
- (43) Neta, P.; Meisel, D. *J. Phys. Chem.* **1976**, *80*, 519.
- (44) Brière, R.; Claxton, T. A.; Ellinger, Y.; Rey, P.; Laugier, J. *J. Am. Chem. Soc.* **1982**, *104*, 34.
- (45) Douady, J.; Ellinger, Y.; Rassat, A.; Subra, R. *Mol. Phys.* **1969**, *17*, 217.
- (46) Imbrota, R.; Barone, V. *Chem. Rev.* **2004**, *104*, 1231.
- (47) Ricca, A.; Tronchet, J. M. J.; Weber, J.; Ellinger, Y. *J. Phys. Chem.* **1992**, *96*, 10779.
- (48) Rhodes et al.¹¹ have studied the effect of this rotation on the hcc-(H, NO•OH) and on the energy. Their results differ from ours on three points: their computed hcc values are all positive, they are all lower than 6.5 G, and a local minimum of energy is obtained when the C–N–O–H dihedral angle equals 0°, roughly 15 kJ.mol⁻¹ higher than the absolute minimum of energy when this dihedral angle equals 180°. From a qualitative

point of view, both types of calculations (DFT and PM3) underestimate the hcc of this proton.

(49) Barone, V.; Bencini, A.; Cossi, M.; Di Matteo, A.; Mattesini, M.; Totti, F. *J. Am. Chem. Soc.* **1998**, *120*, 7069.

(50) Improta, R.; Scalmani, G.; Barone, V. *Chem. Phys. Lett.* **2001**, *336*, 349.

(51) However, our experiments are performed in ethylene glycol which already presents too many degrees of freedom to be treated explicitly here.

(52) We adopted here the terminology, σ versus σ^* , used for sulfur-centered radicals.^{53,54} In σ^* radicals, the N orbitals are hybridized in an sp^3 pyramidal fashion, whereas for σ radicals, the singly occupied molecular orbital (SOMO) main contributor to the (direct) spin delocalization effect⁵⁵ lies in the plane defined by the N and its nearest neighbors.

(53) Chatgililoglu, C. Free radical chemistry of sulfenic acids and their derivatives. In *The Chemistry of Sulphenic Acids and Their Derivatives*; Patai, S., Ed.; John Wiley & Sons Ltd: New York, 1990; p 549.

(54) Pogocki, D.; Schöneich, C. *J. Org. Chem.* **2002**, *67*, 1526.

(55) Adamo, C.; Barone, V.; Subra, R. *Theor. Chim. Acta* **2000**, *104*, 207.

(56) To definitely rule out the possibility for radical **6** to be in fact **k**, many other conformations of **k** were studied by defining paths in the conformational space, i.e., by monitoring the dihedral angles C2–N–O–H and C1–C2–N–OH during geometry optimization. None of the calculated sets of hcc values (data not shown) was compatible with the experimental spectra attributed to radicals **6** and **6d**.

(57) Gronchi, G.; Tordo, P. *Res. Chem. Intermed.* **1993**, *19*, 733.

(58) Thomas, J. R. *J. Am. Chem. Soc.* **1964**, *86*, 1446.

(59) Cauquis, G.; Genies, M.; Lemaire, H.; Rassat, A.; Ravet, J. P. *J. Chem. Phys.* **1967**, *47*, 4642.

(60) Alberti, A.; Barbaro, G.; Battaglia, A.; Guerra, M.; Bernardi, F.; Dondoni, A.; Pedulli, G. F. *J. Org. Chem.* **1981**, *46*, 742.

(61) Hüttermann, J. *Int. J. Radiat. Biol.* **1970**, *17*, 249.

(62) Hole, E. O.; Sagstuen, E.; Nelson, W. H.; Close, D. M. *J. Phys. Chem.* **1991**, *95*, 1494.

(63) Catterall, H.; Davies, M. J.; Gilbert, B. C. *J. Chem. Soc., Perkin Trans. 2* **1992**, 1379.

(64) Wetmore, S. D.; Boyd, R. J.; Eriksson, L. A. *J. Phys. Chem. B* **1998**, *102*, 5369.

(65) Gilbert, B. C.; Norman, R. O. C.; Placucci, G.; Sealy, R. C. *J. Chem. Soc., Perkin Trans. 2* **1975**, 885.

(66) Edge, D. J.; Norman, R. O. C. *J. Chem. Soc. B* **1970**, 1083.

(67) In contrast with radical **s1**, **s2** was not reported in several recent TR-EPR studies involving ethylene glycol as a solvent.^{42,68,69} In steady-state photolysis⁷⁰ and rapid mixing studies,⁷¹ spectra exhibiting a main 1:2:1 triplet were reported. However, hyperfine splitting constants reported in those papers (19.0 and 18.4 G, respectively), differ from that of radical **s2**, and the cited authors attributed them to other radicals (the main hypothesis reported was $H_2C^*(CHO)$).

(68) Li, G. Z.; Li, X.; Zhai, L.; Zheng, L.; Lu, T. X.; Sun, W.; Cui, F. *Colloids Surf., A* **2000**, *167*, 143.

(69) Mu, J. H.; Li, G. Z.; Tu, X. H.; Lu, T. X.; Zhao, K. S. *Chem. Phys. Lett.* **2002**, *354*, 186.

(70) Livingston, R.; Zeldes, H. *J. Am. Chem. Soc.* **1966**, *88*, 4333.

(71) Dixon, W. T.; Norman, R. O. C. *J. Chem. Soc.* **1963**, 3119.

(72) Another hypothesis is the 3-hydroxy-2-nitrophenoxy radical, which could be formed by abstraction of a hydrogen atom from a hydroxyl group of 2-nitrosorcinol. It was ruled out by comparison with experimental hcc⁷³.

(73) Stone, T. J.; Waters, W. A. *J. Chem. Soc.* **1964**, 4302.